RELATIONSHIP BETWEEN PECVD SILICON NITRIDE FILM COMPOSITION AND SURFACE AND EDGE PASSIVATION

Florence Chen[1*], Ingrid Romijn[2], Arthur Weeber[2], Jason Tan[3], Brett Hallam[1], and Jeffrey Cotter[1]
[1]ARC Centre of Excellence for Advanced Silicon Photovoltaics and Photonics, University of New South Wales, Sydney, NSW 2052, Australia. [*]Tel: +61 2 9385 6057, Fax: +61 2 9662 4240, email: florencewchen@gmail.com
[2]ECN Solar Energy, P.O.Box 1, 1755 ZG Petten, The Netherlands
[3]Faculty of Engineering and Information Technology, Australian National University, Canberra, Australia

ABSTRACT: The relationship between film composition and surface passivation provided by PECVD silicon nitride is investigated in this work. Various surface types and planes of n-type float zoned wafers were studied: planar (100), planar (111), textured (random upright pyramids with (111) facets), boron-diffused layer on planar (100) surfaces, and the edges intersecting the p-n junction. The relationship between film composition and surface passivation on planar (100) p-type silicon is also presented. Light soaking and thermal treatments were performed on the samples and the relationship between film composition and stability is briefly explored. It is shown that, with optimised film composition, SiN layers can provide excellent and stable passivation on all surface types investigated in this work. Implied open circuit voltage of more than 700mV and boron emitter dark saturation currents as low as 5 fA/cm^2 are demonstrated.
Keywords: Passivation, Silicon-Nitride, PECVD

1 INTRODUCTION

Silicon nitride (SiN) is widely used in the fabrication of silicon solar cells to increase their efficiency. For example, it is used as an anti-reflection coating (ARC), due to its tuneable refractive index and good optical properties. In multi-crystalline silicon solar cells, SiN provides both bulk and surface passivation by hydrogenating volume defects and dangling bonds at the surface. Recent research efforts have examined the relationship between the film composition and its passivation properties. For example, a study by Mäckel and Lüdemann [1] shows that at as-deposited conditions, good surface passivation is achieved with SiN films that have high Si-H bond density.

However, industrially manufactured solar cells often include a firing step after the deposition of SiN. The bulk passivation quality after firing is a subject of interest to the industry. A study by Hong *et al.* [2] suggests that the final bulk passivation quality increases as the mass density of the SiN films increases. The study showed that a higher amount of hydrogen loss after firing does not necessarily correlate to a better final bulk passivation. This is because films with lower mass densities have more open structures that facilitate the effusion of hydrogen from the film into the ambient [2, 3].

Weeber *et al.* [4,5] and Romijn *et al.* [6] showed a correlation between the Si-N bond density and the surface and bulk passivation quality. Since the Si-N bond density is directly correlated to the mass density of the SiN films, the results are in good agreement with Hong *et al*. Romijn *et al.* found an optimum Si-N bond density of 1.2-1.3x10^{23} cm^{-3} for passivation of multi-crystalline wafers after firing. The studies also showed that the H diffusion is slower in films with high Si-N bond density. As a result, little hydrogen can reach the bulk to provide good defect passivation.

Numerous other studies on similar topics have emerged since then (for example, see ref [6-12]), and it appears that all of the results agree that the mass density or the Si-N bond density (both are inter-related) is one of the key film composition parameters that determines the final passivation quality.

Most of the aforementioned studies focus on the passivation for multi-crystalline silicon solar cells, and where surface passivation is concerned, only one type of surface (namely p-type (100) planar) was studied. The work presented in this paper is an extension of previous studies, with a primary focus on the surface passivation for several key surface types. The surfaces investigated in this work include: n-type planar (100), planar (111), textured (random upright pyramids with (111) facets), and boron-diffused surfaces on n-type (100) silicon. The study on the planar (111) surfaces allows some insight on the surface passivation of textured surfaces (initially (100) surfaces), which have multiple exposed (111) planes. A brief comparison between the surface passivation of n-type and p-type planar (100) surfaces is also presented in this paper.

In addition to surface recombination, edge recombination can also play a significant role in limiting silicon solar cell performance, especially for high efficiency/small-area solar cells. For industrial solar cells, edge isolation is usually done by lasers or by plasma etching, and the edges are often left exposed and unpassivated. The literature on edge passivation, especially by CVD films, is scarce. Therefore a study on the edge passivation by PECVD SiN is included in this work. Some initial results are presented in this paper.

Lastly, stability under thermal annealing and illumination are two important factors that should be considered when incorporating SiN films in solar cells. In this work, samples were fired multiple times to assess their thermal stability. Light soaking was also performed, and the relationship between film composition and stability was briefly explored.

2 EXPERIMENTAL DETAILS

Two different Roth&Rau microwave remote PECVD systems were used to deposit the SiN films in this work: a laboratory-type static deposition system, AK400, at UNSW; and a pilot industrial-type deposition system that is similar to a SiNA XS at ECN. Process parameters such as process pressure, total gas flow,

deposition temperature, and gas flow ratio were varied in order to achieve a range of film compositions. The samples deposited at UNSW and ECN were RCA cleaned and ECN cleaned [13], respectively, followed by an HF dip prior to the depositions.

Float zoned (FZ) wafers were used for the surface passivation study. The type, bulk resistivity, thickness, and surface morphology of the wafers are summarised in Table I.

Table I: A summary of the wafers used in this work.

	Type	Bulk Res. (ohm.cm)	Thickness (µm)	Surface
(100)	n	1	290	DSP*
(100)	p	1	290	DSP*
(111)	n	1	250	CP [14]
Textured	n	1	230	Textured
Boron	n	1	240	SDE+

*DSP=double-side polished; +SDE=saw-damage etched

For boron-diffused samples, boron emitters with a sheet resistance of 60 ohm/sq were formed by borosilicate glass formation at 960°C for 50 minutes, followed by a short low temperature dry oxidation. The borosilicate glass was then stripped off, and a 90-min high temperature dry oxidation was performed. Both sides of the wafers were diffused and oxidized, resulting in a SiO_2-passivated $p^+/n/p^+$ structure. The SiO_2 was then stripped off in 7:1 buffered HF, followed by a RCA clean and a HF dip, and SiN was deposited on both sides of the samples.

For the edge passivation study, a Nd:YAG laser was used to scribe a square isolation trench through the emitters of a separate batch of SiO_2-passivated, boron-diffused samples to define the device active area and isolate the emitters from the physical edges of the wafer. This isolation trench was etched with NaOH to remove laser damage and slag. The SiO_2 was not stripped off in HF, and SiN was deposited on top of the SiO_2, such that the only area passivated by the SiN is the isolation trench.

The surface passivation quality was determined by the implied 1-Sun open circuit voltage (V_{oc}) [15] for non-diffused surfaces, and the dark saturation current density (J_{0d}) [16] for diffused surfaces. In some cases, the surface recombination velocity (SRV) at injection level 10^{15} cm^{-3} was also extracted, assuming infinite bulk lifetime, which gives the upper limit of SRV. These data were extracted from the injection-level dependent lifetime (IDL) data, measured using the quasi-steady-state (QSS) photoconductance (PC) technique [15, 17]. The edge passivation quality was determined by the extended analysis of IDL data measured by QSS photoluminescence (PL) technique, as outlined in ref [18].

The film composition was characterised by FTIR spectroscopy. A separate set of n-type, FZ, 1000 ohm.cm, double-side polished wafers were used for FTIR study at UNSW; while a separate set of p-type, Czochralski (CZ), 1 ohm.cm, double-side polished wafers were used for FTIR study at ECN. These samples were deposited in the same run as the samples used for surface passivation study. A clean reference substrate from each wafer was used to measure the baseline transmission spectrum. The absorption coefficient k was calculated by subtracting the baseline transmission from the sample transmission spectra. The Si-N, Si-H, and N-H bond densities of the films were then extracted by integrating the area under each of the corresponding absorption peaks, and multiplying the area by the appropriate constants. The hydrogen content is calculated using the following formula [1]:

$$\text{H content} = ([\text{Si-H}] + [\text{N-H}]) / ([\text{Si-N}] + [\text{Si-H}] + [\text{N-H}])$$

3 NON-DIFFUSED SURFACES

Previous studies have shown that the Si-N bond density of SiN films is a key parameter that determines the passivation quality. Thus, the results presented in this paper focus on the relationship between the Si-N bond density and the surface passivation quality. Other parameters such as Si-H, N-H, and hydrogen concentration are also briefly investigated.

3.1 N-type Surfaces

The relationship between Si-N bond density and surface passivation quality of various n-type silicon surfaces at as-deposited conditions is shown in Figure 1. The SiN films were all deposited at UNSW using the Roth&Rau AK400 system.

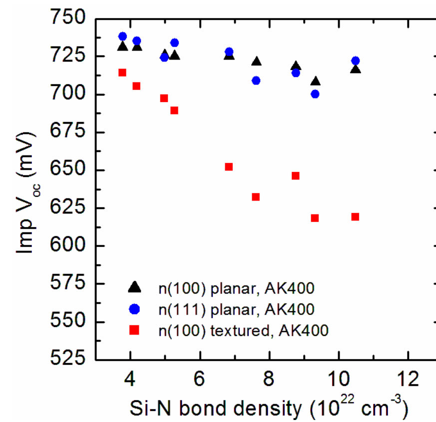

Figure 1: Relationship between the Si-N bond density and the surface passivation quality (as indicated by implied V_{oc}) for n-type, planar (100), planar (111), and textured (random upright pyramids with (111) facets) surfaces at as-deposited conditions.

The extracted upper limit of the SRV of the samples ranges from ~7-12 cm/s at the injection level 10^{15} cm^{-3}, and the extracted implied V_{oc} ranges from 700-730 mV. As shown in Figure 1, the as-deposited SiN films with low Si-N bond densities provide better surface passivation. The low Si-N bond densities also suggest that these films also have lower mass densities and have more open structures [2-3]. There is little difference between the surface passivation quality of the planar (100) and (111) samples for the range of Si-N bond densities investigated. The surface passivation quality of the textured samples appears to be more sensitive to the Si-N bond density of the films than on the planar

samples. This could be due to the larger surface area of the textured wafers, which has a higher interface state density. Nevertheless, the area ratio is about 1.73 and it alone cannot explain the measured difference. It is probable that the lower passivation quality in the textured case is due to the large number of edges and vertices produced by the small random pyramids.

The Si-H and N-H bond densities of the samples are plotted against the Si-N bond density in Figure 2. It can be seen that the SiN films with a lower Si-N bond density have a higher Si-H bond density. This is in good agreement with the observation presented in the study by Mäckel and Lüdemann [1]. Furthermore, films with lower Si-N bond density also have more hydrogen content at as-deposited conditions, as shown in Figure 3.

The results imply that for good surface passivation at as-deposited conditions, it is desirable to have low Si-N bond density, high Si-H bond density, and a high amount of hydrogen in the film.

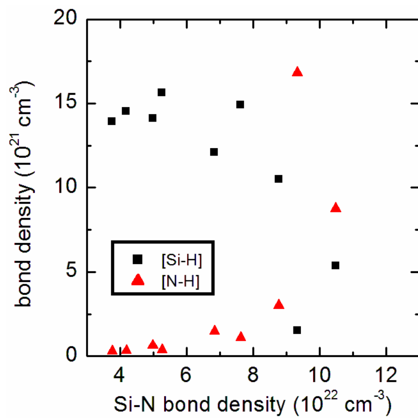

Figure 2: Relationship between Si-N, Si-H, and N-H bond densities for as-deposited films.

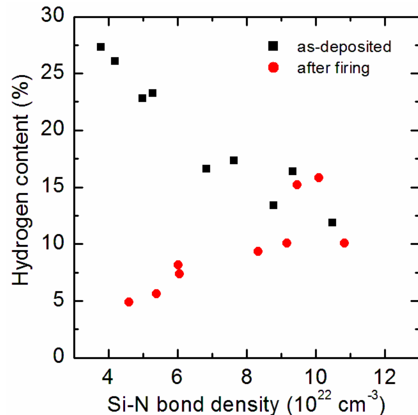

Figure 3: Relationship between Si-N bond density and hydrogen content (in %) for as-deposited and fired films.

The samples were fired in a belt furnace at UNSW. QSS PC and FTIR measurements were taken after firing, and information on the surface passivation quality and the film composition were extracted. It was found that the Si-N bond density of all films increased slightly after firing, which is an indication of densification [2]. The relationship between the Si-N bond density and the surface passivation quality after firing for planar (100), planar (111) and textured surfaces is shown in Figure 4. It can be seen that after firing, all three surface types exhibit the same trend against the Si-N bond density and this trend is very different from the as-deposited case. For the samples with the optimised film composition, the extracted upper limit of the SRV at injection level 10^{15} cm^{-3} is ~7 cm/s.

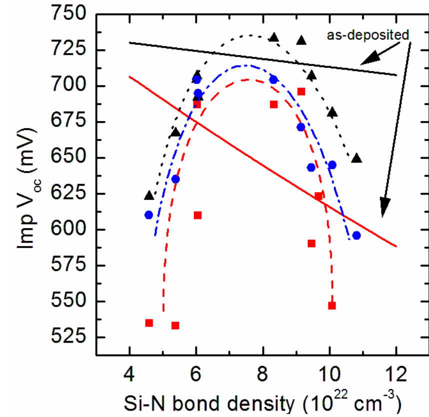

Figure 4: Relationship between the Si-N bond density and the surface passivation quality (as indicated by implied V_{oc}) for n-type, planar (100) (▲), planar (111) (●), and textured (upright random pyramids with (111) facets) (■) surfaces after firing. Dashed lines are added to guide the eyes. For comparison purposes, solid lines are added to indicate approximately the imp V_{oc} of the same samples at as-deposited conditions.

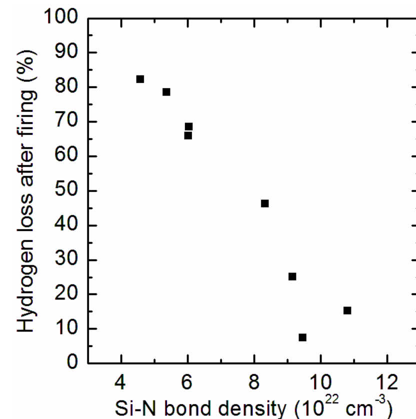

Figure 5: The amount of hydrogen loss plotted against the Si-N bond density after firing.

From Figure 4, we can see that the surface passivation quality decreases significantly for the samples that are coated with SiN films that have low Si-N bond densities. As shown in Figure 5, these films have lost up to ~80% of bonded hydrogen after firing. From literature, the decrease in surface passivation quality can be expected, because the open structure facilitates the formation and effusion of H molecules into the ambient [3]. Interestingly, the samples that are coated with SiN films that have high Si-N bond densities also suffer degradation in the surface passivation quality. As shown in Figure 5, these samples did not lose much bonded hydrogen after firing, although the hydrogen concentration was already relatively low before firing.

The high Si-N bond density implies that these films are relatively dense. Thus, less effusion of H molecules into the ambient can be expected. One possible explanation for the surface passivation degradation is that the bonded hydrogen at the Si-SiN interface dissociated on firing and effused out of the silicon. Since these films had relatively less open structures, the hydrogen from the film was not able to diffuse through the film to replenish the lost hydrogen at the interface. Thus, the surface passivation degraded. However, further investigation is needed to verify this hypothesis.

It is also probable that a different firing profile is required for SiN films with different Si-N bond densities for optimum final surface passivation. Some evidence of this hypothesis is shown in Section 3.2 and Section 5.2.

3.2 P-type Surfaces

A similar investigation was carried out for the p-type planar (100) surface. SiN films were deposited on p-type wafers in the same run as the aforementioned n-type samples in the AK400 system. As shown in Figure 6, the same relationship between the Si-N bond density and the surface passivation quality is also observed on these as-deposited p-type samples. The surface passivation quality on these p-type samples is comparable to that on the n-type samples.

Another set of p-type samples was deposited at 400°C at ECN, using their pilot SiNA XS system. The trends exhibited by both sets of samples deposited in two different machines match up nicely in Figure 6. It should be pointed out that the region where the two sets of data overlap in Figure 6 consists of samples with various refractive indices, ranging approximately from 1.9 to 2.6. On the other hand, the two sets of data do not align in the graph when refractive index is used. This further reinforces the idea that the Si-N bond density is a good alternative way to the refractive index to predict the surface passivation quality.

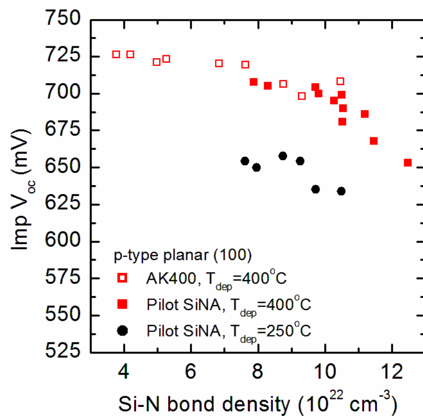

Figure 6: Relationship between surface passivation quality and Si-N bond density for as-deposited p-type planar (100) surface.

A second set of samples was deposited at 250°C at ECN using their pilot SiNA XS system. A similar relationship between the Si-N bond density and the surface passivation quality is also observed for the SiN films deposited at 250°C, but with a lower overall surface passivation quality. The lower surface passivation quality suggests that the thermal history (in this case the deposition temperature) is important for good surface passivation at a given Si-N bond density, and vice versa. The lower surface passivation quality is most likely due to a reduced amount of hydrogen atoms to passivate the interface states at lower temperatures.

The two sets of samples that were deposited in the pilot SiNA XS system were fired at ECN. The results are shown in Figure 7. The surface passivation of these samples increased after firing. In particular, the same relationship between the Si-N bond density and the surface passivation quality can be observed in both sets of samples, which were deposited at two different temperatures but underwent the same post-deposition thermal treatment. This implies that the thermal history is also important in determining the final surface passivation quality at a given Si-N bond density, and vice versa.

The SiN films deposited in the AK400 system were also fired at UNSW. The firing sequence had a longer firing duration and at a lower firing peak temperature than the ECN firing sequence. Contrary to the ECN samples, the surface passivation of these samples all degraded after firing. This further supports the theory that the thermal history is important in the final surface passivation at a given Si-N bond density. It is interesting to note that a similar trend to the fired n-type samples is also observed in these fired p-type samples. However, the fired p-type samples have a slightly broader optimum Si-N bond density in this experiment.

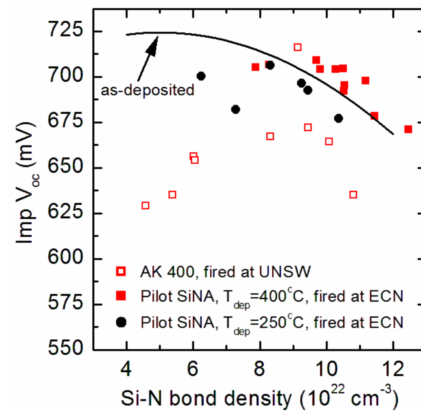

Figure 7: The relationship between surface passivation quality and Si-N bond density of p-type planar (100) surface after firing. For comparison purpose, solid lines are added to indicate approximately the imp V_{oc} of the same samples at as-deposited conditions.

4 DIFFUSED SURFACES AND EDGES

4.1 Boron-diffused Surfaces

Boron-diffused layers are useful as an emitter for n-type solar cells. The ability to passivate boron-diffused surfaces is important for achieving high-efficiency n-type solar cells. Recently, research efforts by various groups [19-22] have been put into PECVD SiN passivation on boron emitters, and good passivation of boron emitters by PECVD SiN was demonstrated [22]. In this work we investigate the relationship between the film composition and the passivation quality on boron emitters.

As shown in Figure 8, there is a relationship

between the Si-N bond density and the passivation quality (indicated by J_{0d}) of 60 ohm/sq boron emitters, for both as-deposited and fired films. The SiN films were deposited and fired at UNSW in the same run as the samples presented in the previous section.

At as-deposited conditions, the SiN films provide poor passivation on boron emitters. However, after firing, the passivation quality of SiN films with Si-N bond density > ~6x10^{22} cm^{-3} greatly improved. J_{0d} as low as 12.5 fA/cm^2 (per side) were achieved after firing with the SiN films that have a Si-N bond density of ~6x10^{22} cm^{-3}.

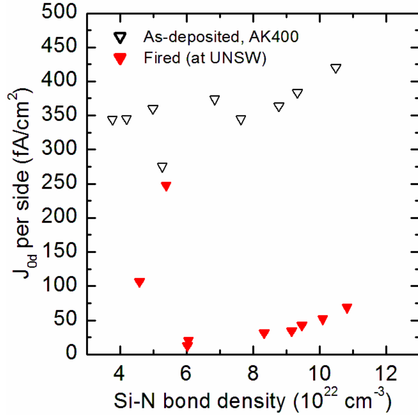

Figure 8: Relationship between surface passivation, represented by the emitter recombination current, and Si-N bond density for boron-diffused surfaces on n-type silicon.

It has been previously shown that the surface passivation provided by SiN on boron emitters is dependent on their sheet resistances [22]. In this work, SiN films with Si-N bond density of ~7x10^{22} cm^{-3} were deposited on boron emitters that have sheet resistances ranging from 45 ohm/sq to 245 ohm/sq. The samples were annealed at 450°C in a N_2 ambient for 240 minutes in a tube furnace (after [22]). The results are plotted in Figure 9. The passivation quality by thermal SiO_2 on the same samples (before the oxide was removed for the PECVD deposition) is also included as a baseline comparison. It can be seen that the passivation quality by PECVD SiN on boron emitters shows a similar dependence on the sheet resistance of the emitters as the thermal SiO_2. For PECVD SiN passivated emitters, J_{0d} of <15 fA/cm^2 (per side) is achieved across the sheet resistance range of 60 ohm/sq to 245 ohm/sq after annealing.

These results demonstrate that SiN is capable of providing good surface passivation on boron emitters when the SiN films have the appropriate Si-N bond density. Note that the best J_{0d} value obtained after a 450°C anneal is practically the same as that measured after a much shorter, higher temperature firing. This indicates that both types of post-deposition thermal treatment have a similar beneficial effect.

The SiN passivation of boron emitters is generally better than that of the baseline SiO_2 passivation in this experiment. However, it should be noted that the passivation quality of the baseline SiO_2 may improve if an alneal is performed. Similarly, the passivation quality provided by both the SiN and SiO_2 may have been better if the anneal was done in a forming gas ambient.

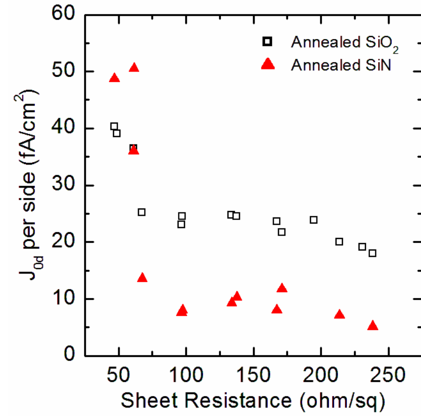

Figure 9: The J_{0d} obtained for boron emitter samples coated with SiN with a Si-N density of ~7x10^{22} cm^{-3} across a range of sheet resistances after annealing. The J_{0d} of thermal oxide passivated samples is included as baseline comparison.

4.2 Edges

Edge recombination can affect the performance of solar cells, especially for small-area and/or high efficiency solar cells. There are two types of edge recombination. Edge-bulk recombination J_{0eb} denotes recombination where the quasi-neutral regions of the device intersect the solar cell's edge, and edge-junction recombination J_{0ej} denotes recombination where the space-charge regions intersect the solar cell's edge. J_{0ej} has an ideality factor of 2, and is one of the main contributors to J_{02} recombination. In this work, the passivation on the edge-junction is explored. J_{0ej} is quantified by applying the circuit analysis and curve fitting method outlined in ref [18]. Typical curve fittings of three different samples for the edge passivation study in this work are shown in Figure 10.

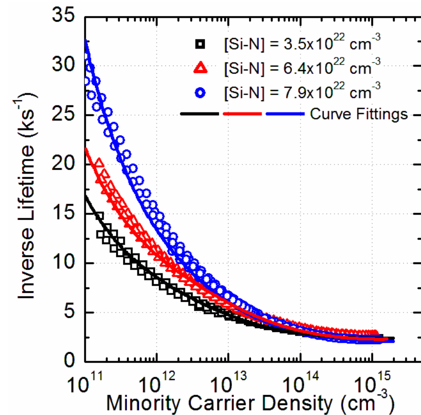

Figure 10: The injection level dependent lifetime curves measured by quasi-steady-state photoluminescence along with the curve fitting from the extended analysis of several samples for the edge passivation study in this work. The method is outlined ref [18].

A relationship between Si-N bond density and edge-junction passivation quality is observed, as illustrated in Figure 11. In general, the data indicates that at as-deposited conditions, the SiN films with low Si-N bond densities provide slightly better edge passivation than the

SiN films with high Si-N bond densities. However the edge passivation quality is poor for all samples at as-deposited conditions, with the extracted edge recombination being on the order of 10^{-9} A/cm. The samples were annealed at 450ºC for 5 minutes in a N_2 ambient. No significant edge recombination was detected after annealing, meaning all of the SiN films are now providing adequate edge passivation, even for a 1-cm^2 high efficiency solar cell. The edge recombination after annealing is estimated to be <~10^{-13} A/cm, which is the detection limit of the method applied to quantify the J_{0ej}.

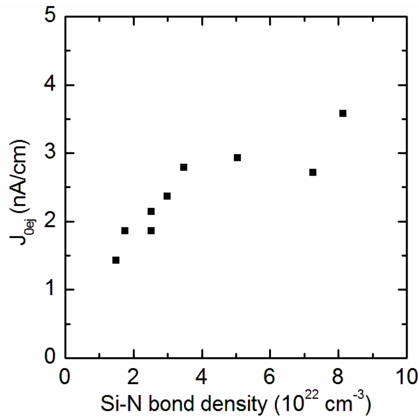

Figure 11: The relationship between edge-junction passivation, expressed by a linear saturation current density, and Si-N bond density at as-deposited conditions. After annealing the J_{0ej} decreased below the detection limit.

5 STABILITY

5.1 Light Stability of As-deposited Samples

The stability under illumination for as-deposited samples was studied. A separate set of n-type planar (100) samples were deposited in the AK400 system at UNSW. They were subjected to light soaking at 1-Sun, 25ºC conditions. The light soaking was performed in various time-interval steps for a total of 8 hours. The evolution of the surface passivation provided by three different SiN films (out of a total of the nine different SiN films studied) is shown in Figure 12.

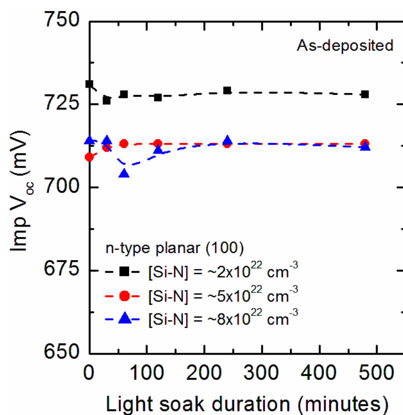

Figure 12: The evolution of surface passivation of three different samples under 1-Sun illumination at 25°C. Dashed lines are added to guide the eyes.

It is interesting to note the initial drop and subsequent recovery in surface passivation on the sample coated with a high Si-N bond density film. The surface passivation mostly recovered after the first initial drop. This behaviour is unlikely to be caused by a structural change in the film, given that the temperature of the sample was kept at 25ºC during light soaking. In addition, the formation of the B-O complex can be ruled out because n-type FZ wafers were used. Nevertheless, the results show that all nine samples have less than ±0.5% change in the implied V_{oc} after 8 hours of light soaking.

5.2 Thermal and Light Stability of Fired Samples

The thermal stability of the surface passivation was investigated. The n-type and p-type planar (100) samples deposited in the AK400 system were fired several more times after the first firing. The implied V_{oc} and film composition were monitored. The thermal behaviour of four representative samples is plotted in Figure 13. As expected, the surface passivation qualities of low Si-N bond density (<~$7x10^{22}$ cm^{-3}) SiN films continue to lose their surface passivation on subsequent firings. The samples coated with medium Si-N density (~7-$9x10^{22}$ cm^{-3}) SiN films experience the classic behaviour of an initial increase and subsequent decrease in surface passivation. Lastly, the samples coated with high Si-N bond density (>~$9x10^{22}$ cm^{-3}) SiN films experience an initial drop followed by a recovery in surface passivation with subsequent firings. In one case, an increase of 30 mV in implied V_{oc} was detected. The recovery in surface passivation was previously reported by Chen *et al.* [23].

The samples were characterised with FTIR after each anneal. These results show that the additional firing sequences further reduced the hydrogen concentration as well as increasing the Si-N bond density of all films. However, the changes observed were relatively small. A similar trend in thermal stability is also observed on the p-type samples.

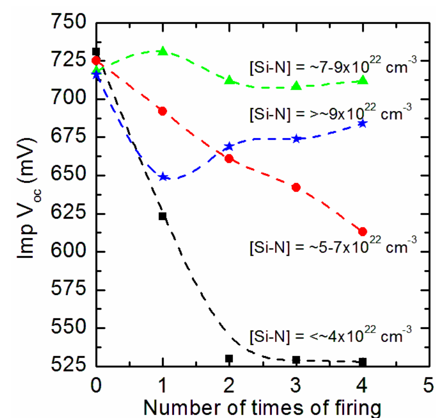

Figure 13: Thermal behaviour of four representative n-type planar (100) samples. Dashed lines are added to guide the eyes.

One hypothesis for the observed thermal behaviour is potential bulk contamination from the belt furnace. A study by Edwards [24] found that some samples had detectable amount of Fe, Ni, Al, Cr, and Ti after going through the belt furnace at UNSW. It is possible that bulk contamination played a part in the initial drop in the

implied V_{oc}, and the contaminants were passivated by hydrogen in the SiN films [25-26] in subsequent firings, thus the recovery in the implied V_{oc} of the samples.

To determine whether Fe may have penetrated into the silicon during firings, the concentration of interstitial Fe (Fe_i) of the wafers was determined following the method proposed by Macdonald *et al.* [27, 28]. Both sets of fired p-type and n-type samples were light soaked for 2 minutes after the multiple firings. The carrier lifetime curves before and after light soaking were compared. A change in the carrier lifetime was observed: some n-type samples experienced an increase in lifetime, while others suffered a decrease in lifetime. In contrast, the lifetimes of all p-type samples increased after illumination. However, we concluded that Fe_i was not responsible for the increased lifetimes as the IDL curves taken before and after illumination did not cross over at injection level $1x10^{14}$ cm^{-3} [28]. Furthermore, the observed change in lifetime after illumination did not revert back to the original state after 48 hours. These results show that Fe and Cr contamination is unlikely.

The SiN films on several representative samples were removed in 49% HF, and the samples were repassivated with a SiN film that is known to provide good surface passivation. Previously unprocessed n- and p-type wafers were included in the deposition run as control samples. After repassivation, the implied V_{oc} of all samples are within 2 mV of their respective control sample. The implied V_{oc} of the control sample are 716 mV and 696 mV for the n-type and p-type wafers, respectively. Therefore we concluded that surface or bulk damage is unlikely.

The repassivated and control samples were also light soaked for 2 minutes. No significant changes in the implied V_{oc} or the lifetime behaviour were observed in these samples. Therefore we concluded that the firing process in this work has led to instability for some films. The observed change in passivation quality after illumination only occurs to samples that were fired in the belt furnace.

It is possible that SiN films with medium Si-N bond density would also experience the recovery effect in surface passivation if the right temperature and time were used. We may have missed the recovery effect of some samples due to the firing temperature and time used in this work. However, the recovery effect is unlikely for the films with low Si-N bond density due to their open structures and high amount of hydrogen loss after the first firing. The differences in the thermal behaviour of SiN films with various Si-N bond densities could explain the trends observed in Section 3, where the high Si-N density films lose surface passivation after firing (see Figure 4 and Figure 7). It is probable that a different firing profile is required for different SiN films to obtain optimum surface passivation.

The relationship between the surface passivation and the Si-N bond density of n-type planar (100) samples after multiple firing and after 2 minutes of light soaking is shown in Figure 14. It can be seen that the relationship changes after multiple firings and after light soaking. After the final processing step, the SiN films that have a high Si-N bond density provide comparable surface passivation quality to the SiN films that have a medium amount of Si-N bonds. From Figure 14, it also appears that the SiN films with a Si-N bond density of $\sim 9x10^{22}$ cm^{-3} are the most stable. The passivation quality of those films did not change significantly after multiple firings and light soaking.

Lastly, the fired boron-diffused samples were also light soaked. No significant changes in the passivation quality or lifetime behaviour were observed. This indicates that the passivation of boron emitters is stable after firing.

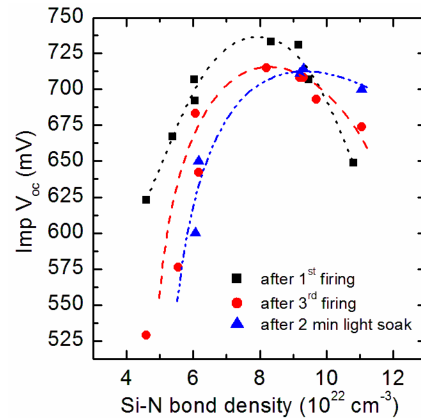

Figure 14: The relationship between the surface passivation and Si-N bond density of n-type planar (100) samples after multiple firings and light soaking. Dashed lines are added to guide the eyes.

6 CONCLUSION

In this work, the relationship between surface passivation and composition of SiN films was investigated. Several key silicon surfaces, including n- and p-type planar (100), n-type planar (111), n-type textured (random upright pyramids with 111 facets), boron emitters, and edges were examined. It was found that the surface passivation quality of all surfaces exhibits a similar trend against Si-N bond density at as-deposited conditions as well as after firing.

At as-deposited conditions, we found that SiN films that have a lower Si-N bond density provide better surface passivation than those with a higher Si-N bond density. These films also tend to have a higher Si-H bond density and hydrogen concentration. The results are in good agreement with the trends observed by Mäckel and Lüdemann [1]. We also showed that the density of SiN films is a good alternative way metric to their refractive indices for the surface passivation, which corresponds well with the results of previous studies. For a given Si-N bond density, the deposition temperature is also important for good surface passivation, and vice versa. Boron emitters and edges are found to be poorly passivated by as-deposited films. The SiN films were found to be stable under illumination, with less than ±0.5% change in the implied V_{oc} after 8 hours of light soaking.

After firing, an optimum Si-N bond density for the final surface passivation exists. For the firing profile used in this work, the optimum Si-N bond density was found to be $\sim 6\text{-}8x10^{22}$ cm^{-3}. We found that for a given Si-N bond density, the post deposition thermal treatment also plays a role in determining the final passivation quality, and vice versa. We showed that SiN films are capable of passivating boron emitters when the films have the

appropriate Si-N bond density and adequate post deposition thermal treatment is given. Dark saturation current densities of <15 fA/cm^2 were achieved on boron emitters with sheet resistances ranging from 60 ohm/sq to 245 ohm/sq, passivated by SiN films that have Si-N bond densities of ~$7x10^{22}$ cm^{-3}. In some cases, J_{0d} of as low as 5 fA/cm^2 is reported. This passivation quality is better than that provided by thermal SiO_2 in this work. The edge passivation provided by all of the SiN films examined in this work improved after a short anneal in N_2 ambient. The dark saturation current densities of the edge-junction were estimated to be < 10^{-13} A/cm after annealing, which is adequate even for small-area solar cells.

On n-type and p-type planar (100) surfaces, three different thermal behaviours were exhibited after multiple firings for SiN films that have different amount of Si-N bond densities. In particular, a recovery in the surface passivation quality was observed on the samples coated with SiN films that have a high Si-N bond density. A change in the surface passivation quality after a short light soak was also noticed for the fired n-type and p-type planar (100) samples. The surface passivation increased for all p-type samples, while some n-type samples experienced an increase and some experienced a decrease in the surface passivation. The exact reason for these changes requires further investigation. However, we have ruled out surface and/or bulk damage. No significant changes in the passivation quality were found after a short light soaking for fired boron-diffused samples. This suggests that the passivation on boron emitters is stable.

7 ACKNOWLEDGEMENTS

This work was produced with the financial assistance of the Australian Research Council (UNSW, ANU) and SenterNovem (ECN). The authors thank Kate Fisher for her assistance in sample preparation, Teun Burgers for his ECN FTIR software, Tsu-Tsung (Andrew) Li for proof reading the paper, and Andres Cuevas for the valuable comments on the paper.

8 REFERENCES

[1] H. Maeckel and R. Luedemann, (2002), J. Appl. Phys., 92 (5), 2602.

[2] J. Hong, W. M. M. Kessels, W. J. Soppe, A. W. Weeber, W. M. Arnoldbik, and M. C. M. van de Sanden, (2003), J. Vac. Sci. Technol. B., 21 (5), 2123.

[3] H. F. W. Dekkers, G. Beaucarne, M. Hiller, H. Charifi, A. Slaoui, (2006), App. Phys. Lett., 89, 211914.

[4] A. W. Weeber, H. C. Rieffe, W. C. Sinke, W. J. Soppe, (2004), Proc. 19th European Photovoltaic Solar Energy Conf., Paris, pp. 1005-1008.

[5] A. W. Weeber, H. C. Rieffe, I. G.Romijn, W. C. Sinke, W. J. Soppe, (2005), 31st IEEE PVSC Conf., Florida, 2005, pp. 1043-1046.

[6] I. G. Romijn, W. J. Soppe, H. C. Rieffe, W. C. Sinke, A. W. Weeber, (2005), 15th Workship on Crystalline Silicon Solar Cells & Modules: Material and Processes, Vail Colarado.

[7] H. F. Dekkers, S. De Wolf, G. Agostinelli, et al., (2004), Technical Digest of International PVSEC 14, Bangkok, pp. 639.

[8] W. M. M. Kessels, P. J. van den Oever, B. Hoex, R. C. M. Bosch, A. J. M. van Emen, M. D. Bijker, and M. C. M. van de Sanden, (2005), 31st IEEE PVSC Conf., Florida, pp. 1253-1256.

[9] A. J. M. van Erven, R. C. M. Bosch, T. Toelle, O. Voigt, S. Petri and M. D. Bijker, (2005), 31st IEEE PVSC Conf., Florida, pp. 947-950.

[10] B. Hoex, A. J. M. van Erven, R. C. M. Bosch, W. T. M. Stals, M. D. Bijker, P. J. van den Oever, W. M. M. Kessels, and M. C. M. van de Sanden, (2005), Prog. Photovolt: Res. Appl. 13, p. 705.

[11] I. G. Romijn, W. J. Soppe, H. C. Rieffe, A. R. Burgers, A. W. Weeber, (2005), Proc. 20th European Photovoltaic Solar Energy Conf., Barcelona, pp. 1352-1355.

[12] S. Winderbaum, I. G. Romijn, D. Sterk, B. van Straaten, (2006), Proc. 21sth European Photovoltaic Solar Energy Conf., Dresden.

[13] C. J. J. Tool, M. Koppes, M. Fleuster, B. H. M. van Straaten, A. W. Weeber, (2006), Proc. 21sth European Photovoltaic Solar Energy Conf., Dresden.

[14] For example, see textbook "Fundamentals of Semiconductor Fabrication", (2003), G.S. May and S. M. Sze.

[15] R. A. Sinton, A. Cuevas, and M. Stuckings, Proc of the 25th IEEE PVSC, pp. 457-460, 1996.

[16] D. E. Kane, and R. M. Swanson, Proc of the 18th IEEE PVSC, pp. 578-583, 1985.

[17] R. A. Sinton, and A. Cuevas, Applied Physics Lett., 69 (17), pp. 2510-12, 1996.

[18] F. W. Chen and J. E. Cotter, (2006), Appl. Phys. Lett., 89, 263509.

[19] M. Kerr, (2002), PhD Thesis, ANU, Canberra.

[20] R. Petres, J. Libal, R. Kopecek, et al, (2005), 15th PVSEC, Shanghai, China.

[21] F. W. Chen, T. A. Li, J. E. Cotter, (2006), 4th World Conference on Photovoltaic Energy Conversion, Hawaii, p. 1020-1023.

[22] F. W. Chen, T. A. Li, J. E. Cotter, (2006), Applied Physics Letter, 88, 263514.

[23] F. W. Chen, J. E. Cotter, A. Cuevas, S. Winderbaum, and K. Roth, (2005), Proc. 20th European Photovoltaic Solar Energy Conf., Barcelona, p.1419-1422.

[24] M. B. Edwards, (2007), PhD Thesis, UNSW, Sydney, to be submitted.

[25] A. Azzizi, L. J. Geerligs, D. Macdonald, (2004), Proc. 19th European Photovoltaic Solar Energy Conf., Paris.

[26] J. Henze, P. Pohl, C. Schmiga, M. Dhamrin, T. Saitoh, I. Yamaga, J. Schmidt, (2006), Proc. 21th European Photovoltaic Solar Energy Conf., Dresden.

[27] D. H. Macdonald, L. J. Geerligs, A. Azzizi, (2004), Journal of App. Phys., 95, 3, 1021-1028.

[28] D. H. Macdonald, T. Roth, P. N. K. Deenapanray, T. Trupke, R. A. Bardos, (2006), App. Phys. Lett., 89, 142107.